HHS Public Access

Author manuscript

Nat Commun. Author manuscript; available in PMC 2015 September 20.

Published in final edited form as:

Nat Commun. ; 6: 6479. doi:10.1038/ncomms7479.

Dietary methionine can sustain cytosolic redox homeostasis in the mouse liver

Sofi Eriksson[1,2,*], **Justin R. Prigge**[1,*], **Emily A. Talago**[1], **Elias S. J. Arnér**[2], and **Edward E. Schmidt**[1]

[1]Microbiology & Immunology, Cooley Hall, Montana State University, PO Box 173520, Bozeman, Montana, USA 59717.

[2]Division of Biochemistry, Medical Biochemistry & Biophysics, Karolinska Institutet, SE-171 77 Stockholm, Sweden.

Abstract

Across phyla, reduced nicotinamide adenine dinucleotide phosphate (NADPH) transfers intracellular reducing power to thioredoxin reductase-1 (TrxR1) and glutathione reductase (GR), thereby supporting fundamental housekeeping and antioxidant pathways. Here we show that a third, NADPH-independent, pathway can bypass the need for TrxR1 and GR in mammalian liver. Most mice genetically engineered to lack both TrxR1 and GR in all hepatocytes ("TR/GR-null livers") remain long-term viable. TR/GR-null livers cannot reduce oxidized glutathione disulfide but still require continuous glutathione synthesis. Inhibition of cystathionine gamma-lyase causes rapid necrosis of TR/GR-null livers, indicating that methionine-fueled *trans*-sulfuration supplies the necessary cysteine precursor for glutathione synthesis *via* an NADPH-independent pathway. We further show that dietary methionine provides the cytosolic disulfide reducing power and all sulfur amino acids in TR/GR-null livers. Although NADPH is generally considered an essential reducing currency, these results indicate that hepatocytes can adequately sustain cytosolic redox homeostasis pathways using either NADPH or methionine.

Introduction

Aerobic metabolism exposes cellular macromolecules to oxidation. To maintain redox homeostasis, most species, including all vertebrates, have two major cytosolic nicotinamide adenine dinucleotide phosphate- (NADPH) dependent disulfide reductase systems: the thioredoxin (Trx) system and the glutathione (GSH) system [1,2]. In mammals, NADPH is generated by glucose oxidation *via* the pentose phosphate pathway or by other oxidases [3–5].

Correspondence and requests for materials should be addressed to E.E.S (eschmidt@montana.edu).

*These authors contributed equally to this submission.

Author Contributions

S.E., J.R.P., E.A.T., and E.E.S. performed the research. Experiments were conceived and designed by S.E., J.R.P., E.S.J.A., and E.E.S. The paper was written by E.S.J.A. and E.E.S. and reviewed by all co-authors.

Competing financial interest

The authors declare that they have no competing financial interests.

Critical homeostasis and cytoprotective reactions that require reducing power from the Trx or GSH systems include the synthesis of DNA precursors by ribonucleotide reductase (RNR), reduction of cystine into cysteine, reduction of protein disulfides, and detoxification of reactive oxygen species [2,6–10].

GSH is a 307 Da tripeptide (L-γ-glutamyl-L-cysteinylglycine) that carries reducing power as a transferrable electron on the thiol (-SH) of the cysteine side-chain [11]. Typically, two GSH molecules oxidize to form glutathione disulfide (GSSG) in reactions that transfer two electrons of reducing power to an acceptor. Glutathione reductase (GR) uses electrons from NADPH to reduce the disulfide bond in GSSG, thereby restoring two molecules of GSH [11]. Mice constitutively lacking GR are robustly viable [12]. Also, although mice constitutively deficient in GSH biosynthesis are embryonic lethal [13], the reasons for lethality are unclear, since mouse cells unable to synthesize GSH are viable in culture [13,14] and organisms of many phyla, including mice, tolerate systemic depletion of GSH [15,16]. Cell or organismal survival in the absence of key components of the GSH system is generally explained by redundancies between the GSH and Trx systems.

Trxs are small proteins (~12 kDa) that carry two transferrable electrons on an active site cysteine-pair *via* a reversible disulfide/dithiol motif. The disulfide can be recycled to a dithiol by Trx-reductase (TrxR), thereby oxidizing one molecule of NADPH [17]. In mammals, the cytosolic Trx system consists of Trx1 and TrxR1. Trx1-null or TrxR1-null zygotes proliferate to contain several thousand viable cells, but they are disorganized and fail to gastrulate [18,19]. Systemic pharmacologic inhibition of TrxR activity in mice or humans is well tolerated [17] and, using conditional alleles to bypass embryonic lethality, it has been shown that TrxR1-null cells and tissues are robust [18,20,21]. TrxR1-null mouse livers require sustained GSH levels to replicate DNA, suggesting that, in the absence of TrxR1, GSH must provide electrons, *via* glutaredoxin, to RNR for synthesis of DNA precursors [10,22]. This further demonstrates a functional redundancy between the Trx1 and GSH systems that allows survival when either one of the systems is compromised.

Although concomitant elimination of both TrxR1 and GSH in hepatocytes blocks DNA replication [10], it has remained uncertain whether reducing power transferred from intracellular oxidative pathways *via* NADPH to the cytosolic disulfide reductase systems is an absolute requirement. Interestingly, mutations compromising NADPH production in humans or mice are often non-lethal, though compensatory pathways remain only partially understood [4,5]. In the current study, to test whether having at least one of the two major cytosolic NADPH-dependent disulfide reductases is essential for hepatocyte survival *in vivo*, we ablated *Txnrd1*, encoding TrxR1, in the hepatocytes of mice having a germline disruption of *Gsr*, encoding GR. We show that mice lacking both TrxR1 and GR in all hepatocytes (“TR/GR-null” livers) can sustain hepatic redox homeostasis and organismal survival using the essential amino acid methionine as the liver’s sole detectable source of both cytosolic disulfide reducing power and sulfur amino acids. This is the first demonstration that an extracellular nutrient, methionine, can supplant the need for intracellular use of NADPH by GR or TrxR1 and sustain cytosolic redox homeostasis in mammalian cells. This study reveals new insights into the diverse mechanisms that cells can

use to maintain redox homeostasis, which may be important during acute oxidative challenge as well as support of basal redox processes.

Results

TR/GR-null livers require *de novo* GSH synthesis for survival

Initial experiments using fluorescently marked mosaic livers revealed that TR/GR-null hepatocytes are stably persistent in mouse livers and that adult mice could survive indefinitely following induced conversion of all hepatocytes to TR/GR-null (Fig. 1). Therefore we generated mice being constitutively whole-liver TR/GR-null (Fig. 2). Despite having neither GR nor TrxR1 in any hepatocytes, these mice exhibited no lethality prior to postnatal day-32 (P32). In most cases, liver histology of post-weaning juveniles (P21 - P32) was grossly normal (Fig. 2a–d), although some animals exhibited possible oval cell expansions (Fig. 2d, white arrow) or small necrotic or leukocytic foci (Fig. 2e, green or yellow arrows, respectively). In animals over 50 days of age, liver histology usually showed leukocytic foci and biliary hyperplasia (Fig. 2f, yellow and black arrows, respectively), suggesting they were surviving under a state of chronic low-grade hepatic inflammation. Between P32 and P42, mice with TR/GR-null livers exhibited 15% spontaneous lethality, which was associated with global liver necrosis; however almost no lethality occurred thereafter (Fig. 2g). Adult mice with TR/GR-null livers were fertile in both genders, although females were somewhat less fecund than controls (70% litter size, Fig. 2h). Liver mass in adults was 2.1-fold greater than controls (Fig. 2i). Immunoblots on liver samples verified that TR/GR-null livers had almost no TrxR1 protein but normal levels of Trx1 (Fig. 3a). Residual TrxR1 in the tissue lysate is likely derived from non-hepatocyte cell types such as endothelia, as shown previously with conditional TrxR1-knockout livers [10,20,23]. TR/GR-null liver lysates also had no detectable NADPH-dependent GSSG reduction activity (Fig. 3b), verifying there was not an alternative NADPH-dependent GSSG reductase supporting homeostasis. TR/GR-null livers had normal concentrations of total glutathione and, surprisingly, most of this was in the reduced (GSH) form (Fig. 3c). By contrast, total proteins from TR/GR-null livers contained only 85% as many reactive thiols as did those from wild-type livers, suggesting that proteins were more oxidized in the TR/GR-null livers (Fig. 3d). During post-hepatectomy regeneration, hepatocyte S-phase indexes were similar in wild-type and TR/GR-null livers (Fig. 3e). However buthionine sulfoximine (BSO), which blocks GSH synthesis, inhibited hepatocyte DNA replication in TR/GR-null livers but not in control livers (Fig. 3e).

Methionine is the precursor of cysteine in TR/GR-null livers

Because TR/GR-null hepatocytes required GSH synthesis for DNA replication but could not reduce GSSG, we inferred that cytosolic disulfide reducing power came from *de novo* synthesis of GSH used in single-turnover reactions. With no ability to reductively recycle GSSG back into GSH, the TR/GR-null hepatocytes would need to excrete the GSSG, which was indeed the case (see below). However, it remained unclear how the hepatocytes would obtain the cysteine precursor required for GSH production. The oxidizing environment of blood plasma rapidly oxidizes cysteine, which is therefore typically transported into cells as its disulfide form, cystine [11]. Subsequently, cystine needs to be reduced intracellularly by

the Trx- or the GSH-system to yield cysteine [8,11]; but both of these systems are disrupted in TR/GR-null hepatocytes. By contrast, the methionine cycle and *trans*-sulfuration pathway, in combination (MTS), can convert the essential amino acid methionine into cysteine without a disulfide reduction reaction [24,25].

To test whether MTS was supporting the TR/GR-null livers, we treated mice with single-dose challenges by inhibitors of cystine uptake (sulfasalazine, SSZ), possible cysteine uptake (2-aminobicyclo-(2,2,1)-heptane-2-caroxylic acid, BCH), conversion of methionine into cysteine by MTS (propargylglycine, PPGG, which inhibits *trans*-sulfuration and not the methionine cycle), or synthesis of GSH (BSO) [11]. Although neither SSZ nor BCH affected mice with TR/GR-null livers (Fig. 4a,b, red lines), a single dose of either PPGG or BSO caused rapid deterioration of these mice (Fig. 4c,d red lines). None of the inhibitors affected control mice having an active allele of *Txnrd1* (Fig. 4a–d, black lines). This revealed that both MTS-based cysteine synthesis and *de novo* GSH synthesis were continuously required to complement the TR/GR-null hepatocytes. Histological analyses revealed that BSO or PPGG treatment induced global necrosis of TR/GR-null livers (Fig. 4e–g).

Next we performed metabolic radiolabeling experiments with either [^{35}S]methionine or [^{35}S]cystine. Using either amino acid, a metabolite was radiolabeled in control livers that migrated as GSH in thin layer chromatography (TLC) (Fig. 4h). In TR/GR-null livers, [^{35}S]methionine labeled this metabolite (red arrow), however [^{35}S]cystine did not (blue arrow). Following [^{35}S]methionine labeling, serum metabolites from mice with TR/GR-null livers showed a labeled species that migrated as GSSG in TLC, which was much less abundant in serum of control mice (Fig. 4i). These results suggested the TR/GR-null livers metabolized [^{35}S] from exogenously supplied [^{35}S]methionine, *via* cysteine and GSH, to GSSG, which was then excreted. The results also confirmed that exogenously supplied [^{35}S]cystine was not effectively utilized for GSH synthesis in TR/GR-null livers.

Both methionine and cysteine are required for protein synthesis. After inoculation with either [^{35}S]methionine or [^{35}S]cystine, proteins became radiolabeled in control livers; however only [^{35}S]methionine gave substantial radiolabeling of proteins in TR/GR-null livers (Fig. 4j). In serum, albumin, which is synthesized by hepatocytes and contains 36 cysteine and 7 methionine residues, was radiolabeled by either [^{35}S]methionine or [^{35}S]cystine in control animals, but was only substantially radiolabeled by [^{35}S]methionine in mice having TR/GR-null livers (Fig. 4j, bottom, purple arrow). These results showed that cystine cannot be effectively utilized as a cysteine precursor in TR/GR-null livers.

Discussion

The use of intracellular NADPH by TrxR or GR to drive cytosolic thiol-disulfide exchange reactions in a reducing direction is considered a nearly universal property of living systems. Here we show that mice lacking all GR activity and constitutively also lacking hepatocytic TrxR1 can maintain sufficient hepatic redox homeostasis and intermediary metabolism for long-term survival. Moreover, our data exclude the possibility that alternative NADPH-dependent oxidoreductases make substantial contributions to supporting disulfide reduction reactions in the TR/GR-null livers. For example, in addition to TrxR1, cells contain the

mitochondrial TrxR2 enzyme [17]. Previously we showed that no alternative sources of TrxR activity, including TrxR2, support DNA replication in GSH-depleted TrxR1-null livers [10]. Consistent with this, TR/GR-null livers are metabolically addicted to MTS-driven synthesis of cysteine and *de* novo synthesis of GSH (Figs 3e & 4c,d), highlighting a critical role of GSH in survival of the TR/GR-null livers. The absence of NADPH-dependent GSSG reduction activity (Fig. 3b) and negligible utilization of exogenous cystine by TR/GR-null livers (Fig. 4h,j) further suggest the TR/GR-null hepatocytes lack activities that could, *via* disulfide reduction, generate substantial levels of cysteine as a source of disulfide reducing power or for protein synthesis. Whereas other NADPH-dependent oxidoreductases expressed in livers lacking TrxR1, such as carbonyl reductases or NADPH-quinone dehydrogenase [20,23], might contribute to redox homeostasis in the TR/GR-null livers by reducing non-sulfur substrates, our results suggest that disulfide reducing activities in TR/GR-null livers are not markedly supported by processes other than *de novo* GSH synthesis.

Normal liver exhibits substantial MTS activity, which uses dietary methionine to generate *S*-adenosylmethionine, recycle 5-methyltetrahydrofolate to tetrahydrofolate, and produce substantial amounts of cysteine, the later of which can be used for *de novo* GSH synthesis and protein synthesis [11,24,26] (Fig 5a). In TR/GR-null livers, since the intracellular transfer of reducing power *via* NADPH and GR or TrxR1 was ablated, extracellular methionine became the sole source of cysteine for both GSH as well as protein synthesis, and thus the sole source of sulfur-containing molecules. Moreover methionine, *via* cysteine and GSH, thereby became the sole detectable source of cytosolic disulfide reducing power in TR/GR-null livers (Fig. 5b).

Control and TR/GR-null livers had similar steady state levels of GSH (Fig. 3c), yet 90 min after metabolic labeling with [^{35}S]methionine the TR/GR-null livers contained substantially less [^{35}S] in hepatic GSH pools (Fig. 4h, red arrow). Because the TR/GR-null livers were unable to incorporate [^{35}S] from cystine into GSH (Fig. 2h, blue arrow), we suspect that the relatively low specific activity of the hepatic GSH pool stemmed from a high rate of GSH turnover in these livers. This interpretation is consistent with the appearance of increased levels of [^{35}S]-labeled GSSG in the serum of animals with TR/GR-null livers following metabolic labeling with [^{35}S]methionine (Fig. 4i). Quantitative metabolite flux analyses will be required to better understand how the demands for *de novo* cysteine and GSH biosynthesis in the TR/GR-null livers impact the transit of amino acids through competing pathways.

The long-term survival of mice with TR/GR-null livers indicates that homeostasis, i.e., a sustainable physiological equilibrium, is achieved in the hepatocytes as well as in all organs of these mice. Although steady state levels and redox-status of glutathione is near-normal (Fig. 3c), total protein thiol content is lower in the TR/GR-null as compared to wild-type livers (Fig. 3d), suggesting the redox equilibrium in these livers is more oxidizing. The diminished protein thiol content; susceptibility to perturbations in methionine metabolism; evidence of chronic low-grade hepatic pathology; and occasional spontaneous death in mice with TR/GR-null livers, suggest that homeostasis in these animals is at the “brink of

failure". Future studies on these mice will likely lead to a better understanding of actual hepatocyte redox requirements, especially under conditions of increased oxidative burden.

GR-dependent recycling of GSSG oxidizes one molecule of NADPH and yields two molecules of GSH. By comparison, conversion of methionine to cysteine *via* MTS hydrolyzes three ATP-phosphodiester bonds and consumes one molecule of serine to produce one molecule of cysteine, one molecule of alpha-ketobutyrate, and one molecule of adenosine [27]. Subsequently, GSH synthesis using this cysteine precursor hydrolyzes two more ATP-phosphodiester bonds and consumes one glutamate and one glycine [11]. Thus, in the TR/GR-null livers, cells must use at least 10 ATP-phosphodiester bonds and two molecules each of methionine, glutamate, glycine, and serine to acquire two molecules of GSH (Fig. 5c). All four amino acids used in this process are readily salvaged from plasma. Also, the energy used as ATP in this process is likely conserved by mitochondrial conversion of alpha-ketobutyrate to succinyl-CoA followed by complete oxidation to 4 CO_2 through two transits of the citric acid cycle and generation of ATP by oxidative phosphorylation (Fig. 6). Thereby, utilization of methionine for obtaining reducing power might, surprisingly, be energetically more favorable than the reductive recycling of GSSG by GR. However, the altered flux of amino acids and their metabolites through transporters, cytosolic pools, MTS, and competing pathways when using methionine as the sole source of reducing power might still be more taxing to the cells.

The liver regulates systemic homeostasis of sugars, lipids, amino acids, nucleosides, vitamins, steroid hormones, and other compounds [28], including sulfur- and seleno-amino acids [29], with hepatocyte Trx1- and GSH-systems participating in these processes [11,30]. Here, however, we report that hepatic function and, thereby, organismal survival, is sustained in mice lacking both TrxR1 and GR in all hepatocytes. Dietary methionine is shown to be an adequate source of sulfur amino acids and disulfide reduction power. This reveals how essential cytosolic disulfide reduction systems, at least in liver, can remain functional without using NADPH, illustrating the robustness of redox homeostasis and identifying methionine as an alternative fuel for redox processes.

Methods

Animals

This study adhered to the United States National Institutes of Health and United States Department of Agriculture guidelines for care and use of animals in research. All animal protocols were reviewed and approved by the Montana State University Institutional Animal Care and Use Committee. The alleles used in this study have been published elsewhere, as described in the text. Except where indicated otherwise, all analyses shown were done on mice of either gender between eight- and twelve-weeks of age. Mice were genotyped by PCR using tail-biopsies harvested between P10 and P14. Mice were kept under specialized care conditions, including continuous-flow HEPA-filtered air cages (Tecniplast); sterilized bedding and enrichment; free access to sterilized feed (Picolabs 5058) and sterilized water; and on a 14:10 light:dark cycle. For hydrodynamic delivery of Cre to liver hepatocytes, mice received a single tail-vein injection of lactated Ringer's solution equal to 10% of their body-weight, containing 5 μg of plasmid pCMVpCreSVtx [31]. For Tamoxifen-induced conversion

of all hepatocytes in mice, *ROSA*$^{mT\text{-}mG/mT\text{-}mG}$;*Txnrd1*$^{cond/cond}$;*Gsr*$^{null/null}$; *Alb*$^{ICE/+}$ mice, having an allele of the *Alb*^{ICE} (for *Alb-IRES-CreERT2)* knock-in allele [32] (a generous gift from P. Chambon and D. Metzger, Illkirch, France), in which an internal ribosomal entry site- (IRES-) driven second cistron targeted into the 3' untranslated region of the endogenous *Alb* locus was used to provide strong hepatocyte-specific transcription and translation of the Tamoxifen-inducible CreERT2 protein. Adult mice were administered a single IP dose of 0.5 ml vegetable oil containing 0.5 mg·ml^{-1} 4-OH-Tamoxifen and 1.5 mg·ml^{-1} Tamoxifen free-base, which resulted in complete conversion of all hepatocytes to green. No feed- or water-supplements were used for the data presented.

To assess survival, pups from 20 litters with different parental combinations were followed. Based on Mendelian segregation of alleles, we expected these litters to yield a total of 41 pups with allelic combinations that would generate AlbCre-driven TR/GR-null livers. Genotype-analyses performed on tail biopsies taken at P10-P14 (dark triangle) indicated that 51 pups had TR/GR-null livers. This value did not differ significantly from expected (T-test, $P = 0.295$), suggesting that zygotes having an allelic combination that should yield TR/GR-null livers survived equivalently to their littermates. At tail biopsy, each animal was given a unique identifier and the 51 mice with TR/GR-null livers were followed with daily monitoring thereafter. Losses include all mice that were either found dead or humanely sacrificed upon becoming moribund.

Statistics

Except as indicated, all analyses were repeated at least in triplicate and representative data is presented. Where applicable, the number (n) is given in figures or legends. Quantitative data is presented as averages ± SEM. Significance was tested on pairwise analyses using a Student's T-test with $P \leq 0.05$ indicating significance.

Surgeries and S phase indexes

Partial (2/3) hepatectomies were performed aseptically under isofluroane anesthesia. The median and left lateral lobes were ligated and resected; incisions were sutured; and surface-exposed sutures were secured with VetBond (3M) tissue adhesive [33–35]. Thirty-six hours after hepatectomy, 5-bromo-2'-deoxyuridine (BrdU, 2.5 μmol in saline, Alfa-Aesar H27260) was injected intraperitoneally. Paraffin sections of livers were stained with mouse anti-BrdU-DNA antibody (Sigma-Aldrich, B2531, 1:10) followed by goat-anti-mouse-HRP-conjugated secondary antibody (MP Biomedicals, 55550, 1:3000). S phase indexes represent the ratio of BrdU-stained to un-stained hepatocyte nuclei. Analyses were repeated on 3–5 animals of each condition and >15,000 hepatocyte nuclei were evaluated for each animal [10,33].

Inhibitor studies

Sulfasalazine (SSZ, MP Biomedicals, 02919944, 5 mg · kg^{-1}), 2-aminobicyclo-(2,2,1)-heptane-2-caroxylic acid (BCH, Sigma-Aldrich, A7902, 700 mg · kg^{-1}), propargylglycine (PPGG, Sigma-Aldrich, P7888, 0.5 mmol · kg^{-1}), or buthionine sulfoximine (BSO, Sigma-Aldrich, B2515, 7.2 mmol · kg^{-1}) were dissolved in sterile saline and were administered as a single intraperitoneal inoculum in each case [16,36–39].

Redox assays and immunoblotting

At sacrifice, livers were perfused with saline (cardiac-portal), excised, cut into ~0.3 g pieces, and pieces were either fixed in neutral-buffered formalin for paraffin-embedding and histology or snap-frozen in liquid nitrogen and stored at −80°C [23]. For immunoblots and GSSG-reductase assays, snap-frozen liver pieces were homogenized in 0.8 ml of ice-cold 50 mM Tris-Cl, pH 7.5, 150 mM NaCl, 2 mM EDTA, 1% Trition X-100, 1X protease inhibitor (Pierce #88666) [10,23,33,40]. After pelleting debris, protein concentrations of the clarified lysates were determined by Bradford assay (Thermo Scientific, 23238). Liver proteins (25 μg) were boiled in loading buffer containing DTT and SDS, separated on 4–20% polyacrylamide gradient gels, and transferred onto nitrocellulose membranes [10]. After blocking in 5% non-fat milk, membranes were incubated overnight with anti-mouse-TrxR1 or anti-mouse-Trx1 rabbit sera (each used at 1:4000 dilution, kindly provided by G. Merrill, Oregon State University) followed by goat-anti-rabbit horse radish peroxidase-conjugated secondary antibody and visualization by chemoluminescence (Pierce PicoWest system) [20]. For NADPH-dependent GSSG reduction assays, 50 μg of liver lysate in 10 μl was mixed with 190 μl of reaction mixture containing 1 mM GSSG (Sigma-Aldrich G4626), and 200 μM NADPH (Sigma-Aldrich N7505) in 100 mM potassium phosphate, pH 7.0, 2 mM EDTA [10,23,41]. Absorbance at 340 nm was followed at 30°C using a Versamax plate reader (Molecular Devices). A background control lacking GSSG for each sample was subtracted from sample activities. To measure GSH and GSSG levels [10,42], snap-frozen liver pieces (~0.3 g) were homogenized in 0.8 ml of 10 mM HCl and proteins were removed by adding 5-sulfosalicyclic acid to 1 % ($w \cdot v^{-1}$) followed by centrifugation. For GSSG measurements, 2 μl of 2-vinyl pyridine (98%, Sigma-Aldrich #132292) was added to 100 μl of each supernatant and incubated at room temperature for 1 h to alkylate free thiols prior to reaction. Reaction mixes contained 120 mM NaH_2PO_4, pH 7.4, 5.3 mM EDTA, 0.75 mM 5,5'-dithiobis-(2-nitrobenzoic acid (Sigma D8130), 0.24 mM NADPH, and 1.2 $IU \cdot ml^{-1}$ GR (Sigma-Aldrich G9297), and either 5 μl (GSH+GSSG assay) or 20 μl (GSSG assay) clarified lysate, and were followed at room temperature by absorbance at 412 nm in a Versamax plate reader. Standard curves prepared in parallel contained GSH or GSSG. Liver GSH and GSSG concentrations were calculated by comparison to standard curves assuming 100% recovery at all steps.

Total protein thiol content was determined using 4,4'-dithiopyridine under denaturing acidic conditions to expose buried cysteines and inhibit *ex vivo* oxidation [43–45]. Briefly, snap-frozen liver samples were thawed by homogenization in 3-volumes of ice-cold 10% tricholoroacetic acid. Precipitated macromolecules were collected by centrifugation and were washed three times with 10% trichloroacetic acid. Pellets were dissolved by brief sonication in a volume equivalent to 30-times the starting liver mass of 0.4 M sodium citrate, pH 4.5, 1 mM EDTA, 5% SDS ("protein samples"). An aliquot of each protein sample (2 μl) was transferred into tubes containing 68 μl 0.1 M sodium citrate, pH 4.5, 1 mM EDTA, 0.3% SDS, and 0.5 mM 4,4'-dithiopyridine (Sigma-Aldrich 143057). Samples were mixed and incubated at room temperature for 30 min. Samples received 130 μl of 0.1 M sodium citrate, pH 4.5, 4 M urea and were incubated another 30 min at room temperature. As a standard curve to calculate thiol content, dithiothreitol powder (Gold Biotechnology, DTT50) was freshly dissolved in 0.4 M sodium citrate, pH 4.5, 1 mM EDTA, 5% SDS and a

dilution series from 0 – 3 nmol was prepared and assayed in parallel with samples. Absorbance of each sample was read at 324 nm in a Beckman DU 800 spectrophotometer. The molar concentration of free thiols in each liver protein sample was determined by comparison to dithiothreitol standard curve, correcting for each molecule of dithiothreitol having two thiols. For total protein amino acid content, a separate aliquot of each protein sample (10 μl) was hydrolyzed overnight at 95–100°C in 100 μl of 6M HCl; dried in a Speed Vac; and re-dissolved in 200 μl of 1X PBS. An aliquot of each (10 μl) was diluted with water to 500 μl and mixed with 500 μl hydrindantin solution, freshly prepared by dissolving 0.1 g ninhydrin (Alpha-Aesar 43846) in 7.3 ml dimethyl sulfoxide, adding 2.5 ml 1.65 M lithium acetate, pH 4.5, and then reducing the ninhydrin by adding 200 μl 0.66 M SnCl. To generate a standard curve of known amino acid content, a dilution series from 0 – 34 nmol of alanine (FW 89.1 $g{\cdot}mol^{-1}$; Acros 102831000) in 1X PBS was assayed in parallel with the liver samples. Samples were incubated at 100°C for 10 min and cooled on ice. Under these conditions, the hydrindantin reacts with the primary amine group on each amino acid giving a blue color that was quantified by absorbance at 570 nm [43]. To calculate the number of thiols per total amino acids in the liver samples, the moles of thiols per volume of each protein sample was divided by the moles of amino acids per volume of the same sample.

Metabolic labeling

[^{35}S]methionine and [^{35}S]cysteine were purchased from MP Biomedicals (MP5100405 and MP5100205, respectively). To generate [^{35}S]cystine, the [^{35}S]cysteine (1 mCi) was incubated with an equal-molar amount of fresh hydrogen peroxide overnight at 25°C, quenched in 10 volumes of cystine-free, methionine-free DMEM medium (Sigma-Aldrich, D0422), and stored frozen. Controls on TLC plates showed that nearly all radioactivity migrated as cystine and not as cysteine on these preparations (Fig. 2h, lane c). For all labeling studies shown, mice were inoculated IP with 0.5 ml of methionine-free, cystine-free DMEM containing 0.2 mCi of the indicated labeled amino acid. Animals were sacrificed 45 or 90 min later, as indicated in the text. Blood was collected by clean-draw from the inferior *vena cava* to produce serum; livers were harvested and snap-frozen in liquid nitrogen and stored at −80°C. Liver fragments were thawed and homogenized by sonication in ~ 10-volumes of ice-cold buffer containing 50 mM Tris-Cl, pH 7.5, 150 mM NaCl, 2 mM EDTA, and 1% Trition X-100 [23]. Homogenates were clarified by centrifugation and protein concentrations were determined by Bradford assay. SDS-PAGE protein gels were run with 50 μg of total liver protein or 10 μg of serum protein. Gels were stained with Coomassie, destained, dried, and exposed by autoradiography or phosphorimaging. For metabolite analyses, liver homogenates or serum samples were prepared by homogenization in 50% methanol on ice. Samples were incubated overnight at −20°C and clarified by centrifugation. A portion of the clarified extract was removed to tubes containing 5-volumes of acetone and proteins were precipitated for 2- to 20-hours at −20°C. Samples were clarified by centrifugation at 4°C for 15 min in a microcentrifuge and the clear supernatant was transferred to a new tube. Solvent was removed to completion using a Speed-Vac and the dried metabolite pellet was resuspended in 50% methanol. Samples were spotted onto silica TLC plates (Sigma-Aldrich, Z122785) and were migrated for 16 h using 3:1:1 butanol:acetic acid:water. Metabolites were detected by autoradiography or phosphorimaging. All plates contained non-labeled standards that were visualized after exposure by spraying with

ninhydrin staining solution (1 mg · ml^{-1} ninhydrin) in acetone with 0.5% acetic acid and heating at 50°C until color developed. Standards used to calibrate TLC were L-methionine (Amresco, E801), L-Cysteine (Sigma-Aldrich, C7755), L-cystine (Chem-Impex International, 00088), L-glutathione disulfide (GSSG, Sigma-Aldrich, G4376), and reduced L-glutathione (GSH, ICN Biomedicals, 101814).

Acknowledgements

The authors thank J. Kundert, L. Johns, E. Young, K. Sonsteng, T. Lanzendorf, A. Alshammari, T. Frerk, B. Hisey, B. Reeves, P. Grieco, A. Holmgren, and T. Gustafsson for their contributions to the research or discussions; W. Pretsch, T. Tipple, and L. Rogers for the Gsr^{null} mice; P. Chambon and D. Metzger for the Alb^{ICE} mice; G. Merrill for antibodies; and B. Wiedenheft, S. McKnight, B. Tu, and M. Taylor for commenting on the manuscript. SE was supported in part by a fellowship from the Foundation Blanceflor Boncompagni Ludovisi, née Bildt. This work was funded by grants from the U.S. National Institutes on Aging and the National Cancer Institute (AG004020 and CA152559), the Montana Agricultural Experiment Station, as well as support from the College of Agriculture and the Department of Microbiology & Immunology at Montana State University to EES; and support from Karolinska Institutet and the Swedish Research Council to ESJA. Infrastructure support was provided by an NIH/IDeA award to Montana State University (GM110732). The authors have no competing financial interests and no conflicts of interest. All mouse lines used in this study, as well as all other renewable resources, are freely available for non-profit research upon request unless specifically restricted by another party.

References

1. Holmgren A. The function of thioredoxin and glutathione in deoxyribonucleic acid synthesis. Biochem Soc Trans. 1977; 5:611–612. [PubMed: 332555]
2. Holmgren A. Antioxidant function of thioredoxin and glutaredoxin systems. Antioxid Redox Signal. 2000; 2:811–820. [PubMed: 11213485]
3. van Zwieten R, Verhoeven AJ, Roos D. Inborn defects in the antioxidant systems of human red blood cells. Free Radic Biol Med. 2014; 67:377–386. [PubMed: 24316370]
4. Stanton RC. Glucose-6-phosphate dehydrogenase, NADPH, and cell survival. IUBMB Life. 2012; 64:362–369. [PubMed: 22431005]
5. Fan J, et al. Quantitative flux analysis reveals folate-dependent NADPH production. Nature. 2014; 510:298–302. [PubMed: 24805240]
6. Gon S, Faulkner MJ, Beckwith J. In vivo requirement for glutaredoxins and thioredoxins in the reduction of the ribonucleotide reductases of Escherichia coli. Antioxid Redox Signal. 2006; 8:735–742. [PubMed: 16771665]
7. Prinz WA, Aslund F, Holmgren A, Beckwith J. The role of the thioredoxin and glutaredoxin pathways in reducing protein disulfide bonds in the Escherichia coli cytoplasm. J Biol Chem. 1997; 272:15661–15667. [PubMed: 9188456]
8. Pader I, et al. Thioredoxin-related protein of 14 kDa is an efficient L-cystine reductase and S-denitrosylase. Proc Natl Acad Sci U S A. 2014; 111:6964–6969. [PubMed: 24778250]
9. Arnér ESJ, Holmgren A. Physiological functions of thioredoxin and thioredoxin reductase. Eur J Biochem. 2000; 267:6102–6109. [PubMed: 11012661]
10. Prigge JR, et al. Hepatocyte DNA replication in growing liver requires either glutathione or a single allele of txnrd1. Free Radic Biol Med. 2012; 52:803–810. [PubMed: 22198266]
11. Lu SC. Glutathione synthesis. Biochim Biophys Acta. 2013; 1830:3143–3153. [PubMed: 22995213]
12. Rogers LK, et al. Analyses of glutathione reductase hypomorphic mice indicate a genetic knockout. Toxicol Sci. 2004; 82:367–373. [PubMed: 15342956]
13. Shi ZZ, et al. Glutathione synthesis is essential for mouse development but not for cell growth in culture. Proc Natl Acad Sci U S A. 2000; 97:5101–5106. [PubMed: 10805773]
14. Rojas E, et al. Cell survival and changes in gene expression in cells unable to synthesize glutathione. Biofactors. 2003; 17:13–19. [PubMed: 12897424]

15. Reichheld JP, et al. Inactivation of thioredoxin reductases reveals a complex interplay between thioredoxin and glutathione pathways in Arabidopsis development. Plant Cell. 2007; 19:1851–1865. [PubMed: 17586656]
16. Williamson JM, Boettcher B, Meister A. Intracellular cysteine delivery system that protects against toxicity by promoting glutathione synthesis. Proc Natl Acad Sci U S A. 1982; 79:6246–6249. [PubMed: 6959113]
17. Arnér ESJ. Focus on mammalian thioredoxin reductases--important selenoproteins with versatile functions. Biochim Biophys Acta. 2009; 1790:495–526. [PubMed: 19364476]
18. Bondareva AA, et al. Effects of thioredoxin reductase-1 deletion on embryogenesis and transcriptome. Free Radic Biol Med. 2007; 43:911–923. [PubMed: 17697936]
19. Matsui M, et al. Early embryonic lethality caused by targeted disruption of the mouse thioredoxin gene. Dev Biol. 1996; 178:179–185. [PubMed: 8812119]
20. Suvorova ES, et al. Cytoprotective Nrf2 pathway is induced in chronically txnrd 1-deficient hepatocytes. PLoS One. 2009; 4:e6158. [PubMed: 19584930]
21. Mandal PK, et al. Loss of thioredoxin reductase 1 renders tumors highly susceptible to pharmacologic glutathione deprivation. Cancer Res. 2010; 70:9505–9514. [PubMed: 21045148]
22. Holmgren A. Thioredoxin and glutaredoxin systems. J Biol Chem. 1989; 264:13963–13966. [PubMed: 2668278]
23. Iverson SV, et al. A Txnrd1-dependent metabolic switch alters hepatic lipogenesis, glycogen storage, and detoxification. Free Radic Biol Med. 2013; 63:369–380. [PubMed: 23743293]
24. Fukagawa NK. Sparing of methionine requirements: evaluation of human data takes sulfur amino acids beyond protein. J Nutr. 2006; 136:1676S–1681S. [PubMed: 16702339]
25. Belalcazar AD, Ball JG, Frost LM, Valentovic MA, Wilkinson Jt. Transsulfuration Is a Significant Source of Sulfur for Glutathione Production in Human Mammary Epithelial Cells. ISRN biochemistry. 2014; 2013:637897. [PubMed: 24634789]
26. Mosharov E, Cranford MR, Banerjee R. The quantitatively important relationship between homocysteine metabolism and glutathione synthesis by the transsulfuration pathway and its regulation by redox changes. Biochemistry. 2000; 39:13005–13011. [PubMed: 11041866]
27. Aitken SM, Lodha PH, Morneau DJ. The enzymes of the transsulfuration pathways: active-site characterizations. Biochim Biophys Acta. 2011; 1814:1511–1517. [PubMed: 21435402]
28. Dudrick SJ, Kavic SM. Hepatobiliary nutrition: history and future. J Hepatobiliary Pancreat Surg. 2002; 9:459–468. [PubMed: 12483268]
29. Burk RF, Hill KE. Selenoprotein P-expression, functions, and roles in mammals. Biochim Biophys Acta. 2009; 1790:1441–1447. [PubMed: 19345254]
30. Lu J, Holmgren A. Selenoproteins. J Biol Chem. 2009; 284:723–727. [PubMed: 18757362]
31. Sonsteng KM, Prigge JR, Talago EA, June RK, Schmidt EE. Hydrodynamic delivery of Cre protein to lineage-mark or time-stamp mouse hepatocytes in situ. PLoS ONE. 2014; 9:e91219. [PubMed: 24626158]
32. Schuler M, Dierich A, Chambon P, Metzger D. Efficient temporally controlled targeted somatic mutagenesis in hepatocytes of the mouse. Genesis. 2004; 39:167–172. [PubMed: 15282742]
33. Rollins MF, et al. Hepatocytes lacking thioredoxin reductase 1 have normal replicative potential during development and regeneration. J Cell Sci. 2010; 123:2402–2412. [PubMed: 20571049]
34. Iverson SV, Comstock KM, Kundert JA, Schmidt EE. Contributions of new hepatocyte lineages to liver growth, maintenance, and regeneration in mice. Hepatology. 2011; 54:655–663. [PubMed: 21538442]
35. Mitchell C, Willenbring H. A reproducible and well-tolerated method for 2/3 partial hepatectomy in mice. Nat Protoc. 2008; 3:1167–1170. [PubMed: 18600221]
36. Lu SC. Regulation of hepatic glutathione synthesis: current concepts and controversies. Faseb J. 1999; 13:1169–1183. [PubMed: 10385608]
37. Han SJ, et al. beta-Cell-protective effect of 2-aminobicyclo-(2,2,1)-heptane-2-carboxylic acid as a glutamate dehydrogenase activator in db/db mice. The Journal of endocrinology. 2012; 212:307–315. [PubMed: 22131441]

38. Lin J, et al. L-type amino acid transporter-1 overexpression and melphalan sensitivity in Barrett's adenocarcinoma. Neoplasia. 2004; 6:74–84. [PubMed: 15068672]

39. Lewerenz J, et al. The cystine/glutamate antiporter system x(c)(−) in health and disease: from molecular mechanisms to novel therapeutic opportunities. Antioxid Redox Signal. 2013; 18:522–555. [PubMed: 22667998]

40. Mannervik B, Axelsson K, Sundewall AC, Holmgren A. Relative contributions of thioltransferase- and thioredoxin-dependent systems in reduction of low-molecular-mass and protein disulphides. Biochem J. 1983; 213:519–523. [PubMed: 6351844]

41. Eriksson SE, Prast-Nielsen S, Flaberg E, Szekely L, Arnér ESJ. High levels of thioredoxin reductase 1 modulate drug-specific cytotoxic efficacy. Free Radic Biol Med. 2009; 47:1661–1671. [PubMed: 19766715]

42. Vandeputte C, Guizon I, Genestie-Denis I, Vannier B, Lorenzon G. A microtiter plate assay for total glutathione and glutathione disulfide contents in cultured/isolated cells: performance study of a new miniaturized protocol. Cell Biol Toxicol. 1994; 10:415–421. [PubMed: 7697505]

43. Hansen RE, Roth D, Winther JR. Quantifying the global cellular thiol-disulfide status. Proc Natl Acad Sci U S A. 2009; 106:422–427. [PubMed: 19122143]

44. Ostergaard H, Tachibana C, Winther JR. Monitoring disulfide bond formation in the eukaryotic cytosol. J Cell Biol. 2004; 166:337–345. [PubMed: 15277542]

45. Riener CK, Kada G, Gruber HJ. Quick measurement of protein sulfhydryls with Ellman's reagent and with 4,4'-dithiodipyridine. Analytical and bioanalytical chemistry. 2002; 373:266–276. [PubMed: 12110978]

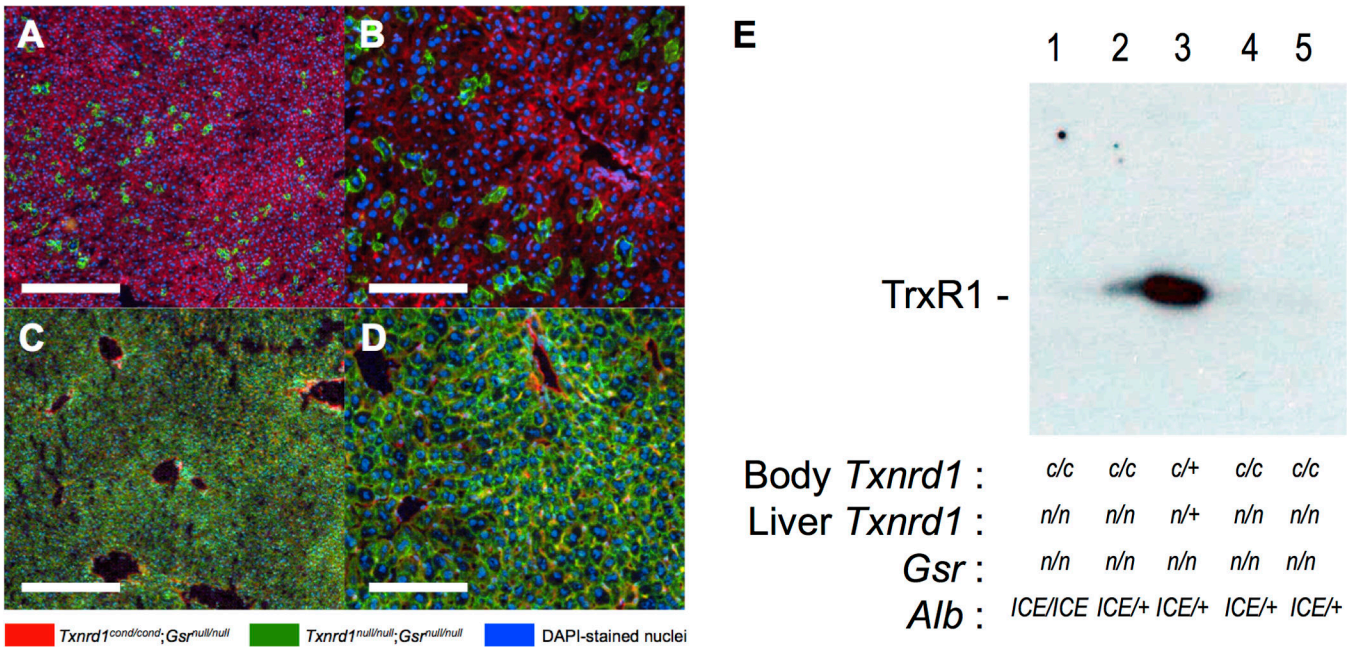

Figure 1. Long-term persistence of TR/GR-null hepatocytes *in situ*

(**a,b**) Fluorescently marked mosaic analysis of TR/GR-null hepatocyte longevity. An arbitrary subset of hepatocytes in adult *ROSA*$^{mT\text{-}mG/mT\text{-}mG}$;*Txnrd1*$^{cond/cond}$;*Gsr*$^{null/null}$ mice were exposed to Cre recombinase by hydrodynamic delivery of plasmid pCMVpCreSVtx, harvested 22 days later, and stained with DAPI. (**c,d**) Survival of livers in which most or all hepatocytes are TR/GR-null. Adult *ROSA*$^{mT\text{-}mG/mT\text{-}mG}$;*Txnrd1*$^{cond/cond}$;*Gsr*$^{null/null}$; *Alb*$^{ICE/+}$ mice, having Cre expression driven by the *Alb*^{ICE} allele received a single IP dose of Tamoxifen. Images shown are DAPI-stained cryosections of livers from mice harvested four weeks after Tamoxifen administration. Scale bars, 200 μm (panels **a**,**c**) or 50 μm (panels **b,d**). (**e**) Immunoblots of TrxR1 protein in livers. Mice received a single dose of Tamoxifen as in **c** and **d**, above, and were harvested ≥16 days later. Each lane contained 75 μg of whole liver lysate. Genotypes of the mouse body and liver are indicated below. Residual TrxR1 protein in lane 2 is due either to incomplete conversion or spill-over from lane 3. Abbreviations, c, conditional-null allele; n, null allele; +, wild-type allele.

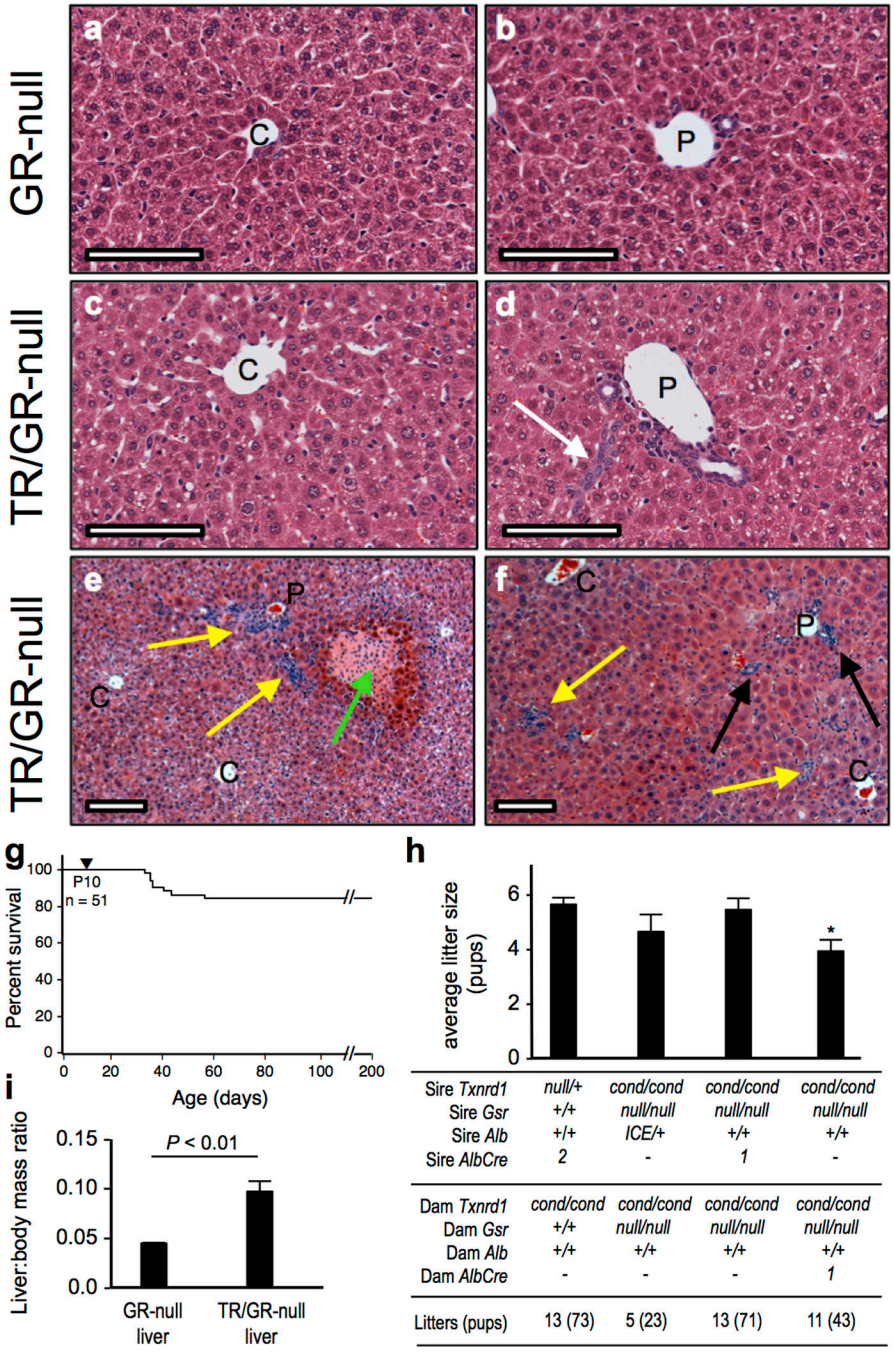

Figure 2. Survival and physiological characteristics of mice with TR/GR-null livers

(**a–f**) Histopathology. As indicated at left, control GR-null livers (**a,b**) or *AlbCre*-driven TR/GR-null livers (**c–f**) are shown from P22 (**a–e**) or P56 (**f**) mice. Higher magnification images show representative centrolobular (**a,c**) or periportal (**b,d**) regions. White arrow, tract of apparent oval cells; yellow arrows, leukocytic foci; green arrow, necrotic focus, black arrow, biliary expansion. C, central veins; P, portal triad. Scale bars 100 μm on all panels. (**g**) Survival of mice with *AlbCre*-driven TR/GR-null livers. Fifty-one pups from 20 litters with AlbCre-driven TR/GR-null livers were followed. No mice were lost before P32.

Between P32 and P42, 15% of the mice were lost. Only one additional loss occurred thereafter (at P55). (**h**) Gender-specific fecundity. Genotypes of sires and dams for each of four mating classes, as well as the number of litters produced and the pups weaned, are indicated at bottom. For a control (first bar from left), production for the TR-null liver colony was monitored over 13 litters (73 pups), giving an average of 5.6 pups/litter. Fecundity was similar in the mice in which Alb^{ICE} drives conversion of livers to TR/GR-null (4.6 pups/litter, second bar from left). Fecundity was also similar in matings where the sires had *AlbCre*-driven TR/GR-null livers and the dams had GR-null livers (third bar from left, 5.5 pups/litter). However, when dams with TR/GR-null livers were mated with sires with *GR-null* livers, production was only 70% (fourth bar from left, 3.9 pups/liter), which was significantly less than the controls ($P < 0.01$). None of the first 3 conditions differed significantly from each other. The five oldest production breeders with TR/GR-null livers in the colony, as of this writing, are all over 365 days old (2 female, 3 male) and in combination have weaned ~30 litters. (**i**) Adult (P49-64) *TR/GR-null* liver size. The liver:body mass ratio was measured for 10 $Txnrd1^{+/+};Gsr^{null/null}$ control and 7 $Txnrd1^{cond/cond};Gsr^{null/null};AlbCre^{1}$ (*TR/GR-null* liver) mice. Bars show mean ± SEM.

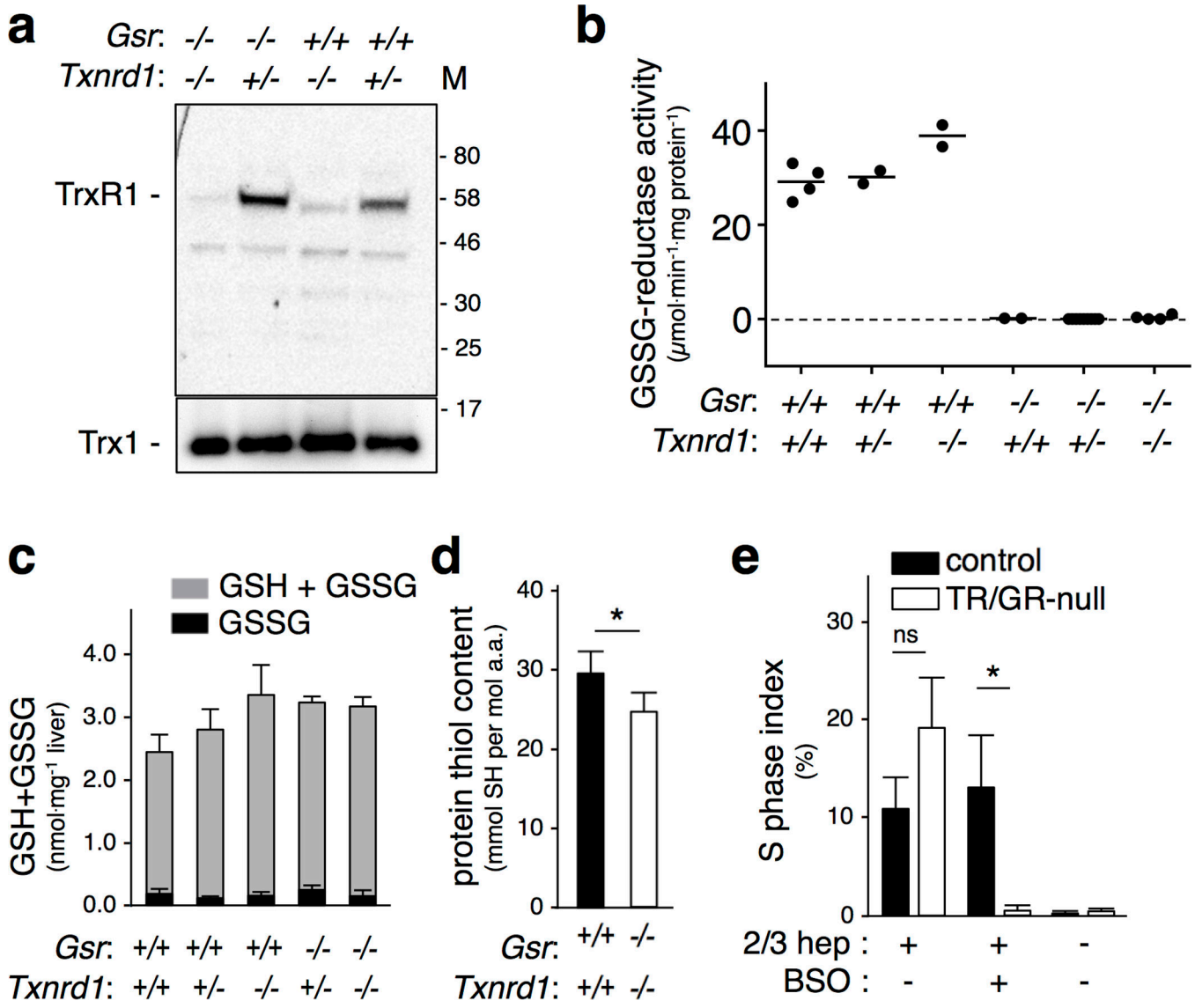

Figure 3. Redox homeostasis in TR/GR-null livers

(**a**) Immunoblots for TrxR1 (top) or Trx1 (below). Hepatocytic genotypes at *Gsr* and *Txnrd1* loci are indicated. M, molecular size markers (kDa). (**b**) NADPH-dependent GSSG-reductase activity. Hepatocytic genotypes at the *Gsr* and *Txnrd1* loci are indicated;each dot represents one animal. (**c**) Hepatic levels of total glutathione (GSH + GSSG) and oxidized glutathione disulfide (GSSG) are shown. n = 4 animals each for wild-type and TR/GR-null livers (first and last bars), and 2–7 animals each for other genotypes; bars represent mean ± SEM. No differences in GSH + GSSG levels were significant, Student's T-test. Mean GSSG values were, from left to right, 0.17, 0.09, 0.15, 0.32, and 0.12 nmol·mg^{-1} liver, respectively. (**d**) Total protein thiol content in wild-type and TR/GR-null livers. Acid-precipitated total liver proteins were resuspended in acidic denaturing buffer and reacted with 4,4'-dithiol pyridine. Comparison to a standard curve was used to quantify protein thiol (SH) content and this was normalized to total amino acid (a.a.) content. n = 9 wild-type and 8 TR/GR-null livers. (**e**) Proliferation rates in regenerating or resting livers. Mice were either 2/3

hepatectomized or not. As indicated, BSO was administered 32 h later and 2 h after that bromodeoxyuridine (BrdU) was administered. Livers were harvested 12 h later and BrdU-labeled (S phase) nuclei were enumerated. n = 3–5 for each condition; graphs show mean and SEM. *, $P \leq 0.05$, Student's T-test.

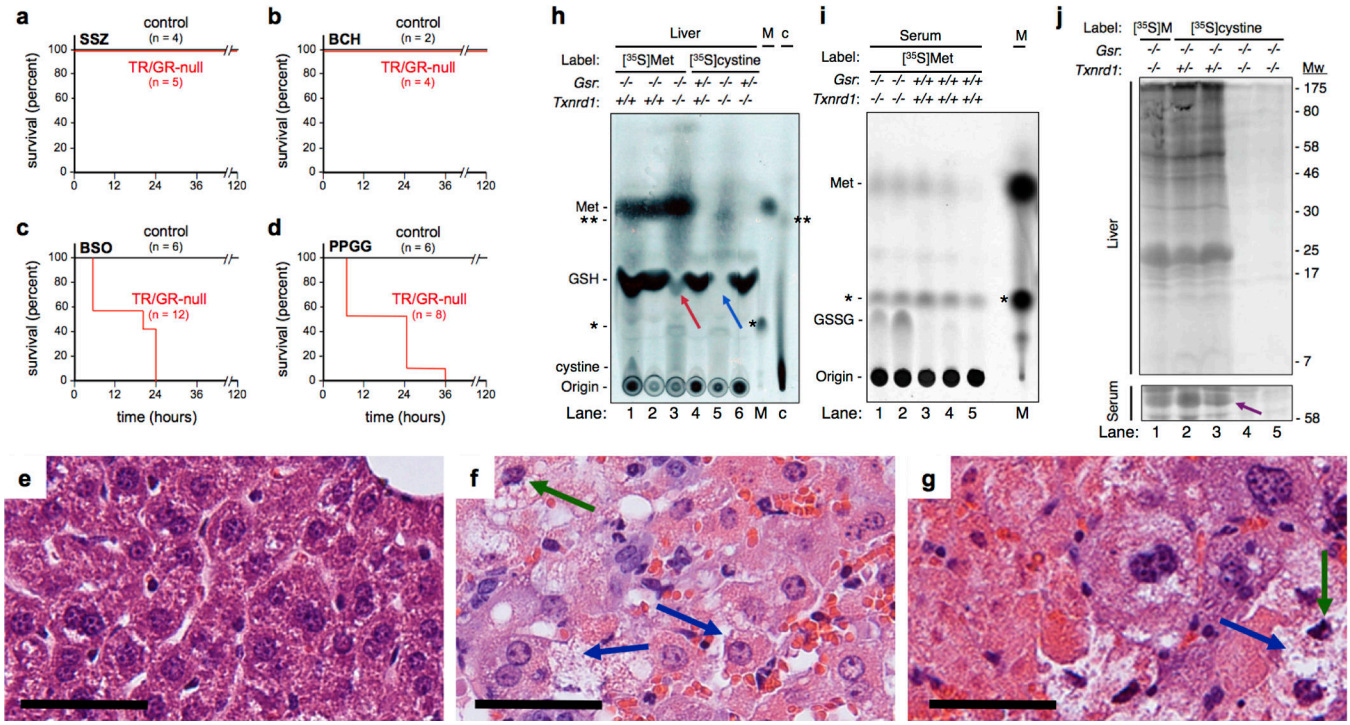

Figure 4. TR/GR-null livers require *trans*-sulfuration

(**a–d**) Adult mice with TR/GR-null livers (genotype *Txnrd1*$^{cond/cond}$;*Gsr*$^{-/-}$;*AlbCre*^{1}; red lines) or controls with one active *Txnrd1* allele (genotype *Txnrd1*$^{cond/+}$;*Gsr*$^{-/-}$;*AlbCre*^{1}; black lines) were treated at time zero with a single dose of SSZ, BCH, BSO, or PPGG, as indicated. (**e–g**), Hematoxylin and eosin-stained histology of TR/GR-null livers following no treatment (**e**), treatment with BSO (**f**), or treatment with PPGG (**g**). Blue arrows, necrotic hepatocytes; green arrows, pyknotic nuclei. Scale bars 50 μm. (**h**) TLC of [^{35}S]-labeled metabolites from livers 90 min after [^{35}S]methionine (Met) (lanes 1–3) or [^{35}S]cystine (lanes 4–6) administration. Lane M, trace of the [^{35}S]Met labeling mix. Asterisk, spontaneous decay product of [^{35}S]Met that migrated slower than GSH but faster than GSSG. Lane c, trace of [^{35}S]cystine labeling mix verifying that most of the label is cystine; little is in the faster-migrating cysteine-form (Cys) (double asterisk). Migration positions of Met, Cys, GSH, GSSG, and cystine standards are indicated at left. (**i**) TLC analysis of [^{35}S]-labeled serum metabolites 45 min after [^{35}S]Met administration. Asterisks as in **h.** (**j**) SDS-PAGE of [^{35}S]-labeled proteins from liver (top) or serum (below) 45 min after [^{35}S]Met (lane 1) or [^{35}S]cystine (lanes 2–5) administration. Mw, molecular-weight markers. Purple arrow, serum albumin.

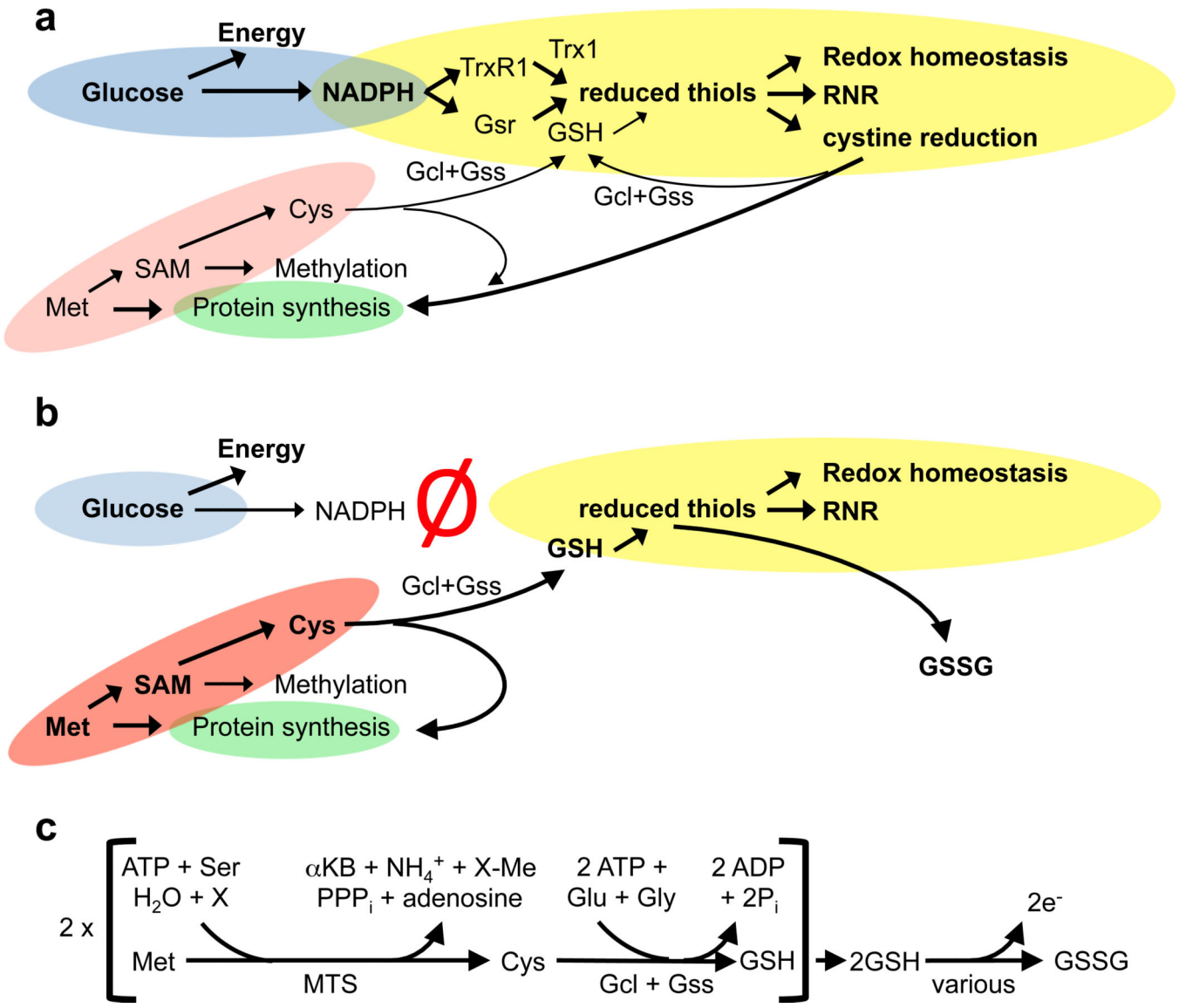

Figure 5. Alternative pathways can maintain redox homeostasis in hepatocytes

(**a**) In normal hepatocytes, glucose utilization by the pentose phosphate pathway (blue) yields NADPH, which feeds the GSH and Trx1 systems (yellow). These systems maintain cytosolic redox homeostasis, drive RNR, and reduce L-cystine into cysteine. MTS (red) supplies SAM for methylation reactions and provides an alternative source of cytosolic cysteine, which is used for protein- (green) and GSH-synthesis. (**b**) Concomitant genetic ablation of GR and TrxR1 (red "Ø") in TR/GR-null livers uncouples glucose oxidation and NADPH from the major disulfide reduction systems. In this case, MTS uses dietary methionine to provide an alternative source of cytosolic cysteine. This cysteine is sufficient to support protein synthesis and to serve as the sole source of cytosolic disulfide reduction power in TR/GR-null livers without the use of NADPH. (**c**) Balanced reaction for utilization of two electrons of reducing power in TR/GR-null hepatocytes. Gcl, glutamate-cysteine ligase; Gss, GSH-synthase; PPP_i, inorganic triphosphate; X, any methyl- (Me-) acceptor for SAM-dependent methyl transferase activity.

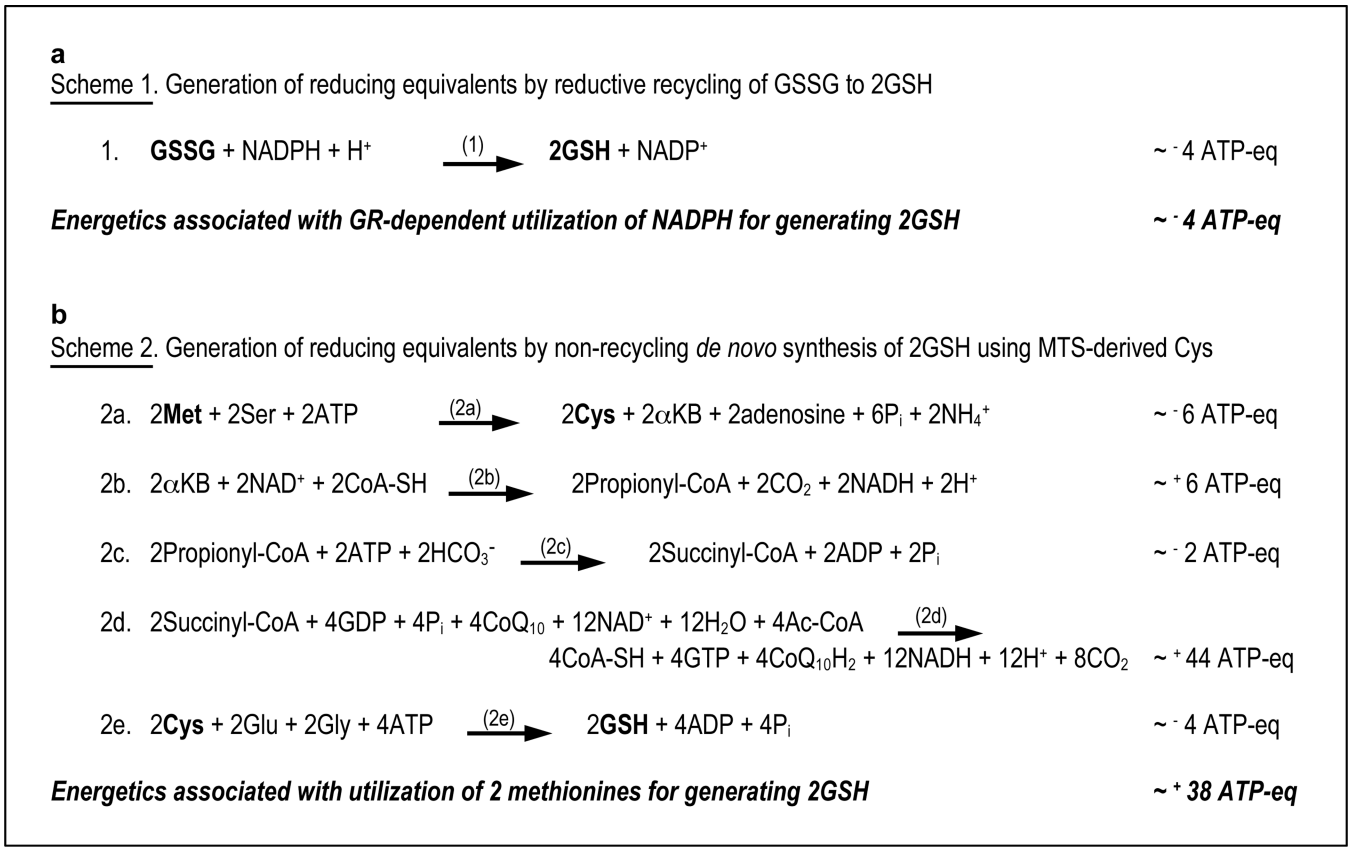

Figure 6. Relative energetics of using intracellular NADPH versus dietary amino acids for reducing power

Schematics are presented for general comparison of the bioenergetics of the alternative sources of GSH discussed in this study, initiating with either NADPH + GSSG in Scheme 1 or with Met + Ser + Glu + Gly in Scheme 2. The energy gain from NADPH production in the PPP is not considered, as this is only one of several catabolic pathways for glucose. Also, no energetic consumption was estimated for acquisition of Met, Ser, Glu, or Gly in reactions 2A or 2E because these amino acids are readily salvaged from plasma. **a,** Scheme 1. Generation of reducing equivalents by reductive recycling of GSSG to 2GSH. **b,** Scheme 2. Generation of reducing equivalents by non-recycling *de novo* synthesis of GSH using Cys synthesized *de novo* from Met. Pathways/enzymes: (1) GR; (2a) MTS; (2b) branched chain alpha-ketoacid dehydrogenase complex; (2c) propionyl-CoA carboxylase, methylmalonyl-CoA racemase, and methylmalonyl-CoA mutase; (2d) citric acid cycle; (2e) Gcl and Gss. Reactions 1, 2a, and 2e are cytosolic; 2b, 2c, and 2d are mitochondrial. Energetic values are given as ATP-equivalents (ATP-eq) and based on estimates of 1 NADPH = 4 ATP; 1 NADH = 3 ATP; 1 $CoQ_{10}H_2$ = 2 ATP; 1 GTP = 1 ATP. Although utilization of 2 Met to obtain 2 electrons of reducing potential consumes 10 ATP-phosphodiester bonds in the primary reactions (2a & 2e), the potential energy yield from mitochondrial utilization of 2 alpha-ketobutyrate, a byproduct of reaction 2a, would make this pathway energetically favorable, with a potential net *gain* of ~ 38 ATP-eq for generating 2 GSH as compared to a

loss of ~ 4 ATP-eq for GR-catalyzed reductive recycling of GSSG to 2 GSH. Metabolites with redox-active sulfurs are in bold-block font.